Res Chem Intermed (2010) 36:155–161
DOI 10.1007/s11164-010-0125-6

Solvothermal synthesis and photocatalytic activity of S-doped TiO_2 and TiS_2 powders

H. Y. He

Received: 31 January 2009 / Accepted: 3 November 2009 / Published online: 4 March 2010

Abstract The photocatalytic activity of S-doped TiO_2 powder depends on the S content. To synthesize S-doped TiO_2 powders with high S content, solvothermal processes were used in this work. The S-doped TiO_2 powder contains 2.0 M% sulfur and has an absorption edge of 460 nm (2.7 eV). The pure TiS_2 powder also synthesized by a solvothermal process has an absorption edge of 595 nm (2.08 eV) and broad absorption above 595 nm. The photocatalysis experiments indicate that the degradation of methyl orange is associated with the light adsorption edge. The photocatalytic activity is much larger for the pure TiS_2 powder than for partially S-doped TiO_2 powder.

Keywords S-doped TiO_2 · TiS_2 · Solvothermal process · Nanocrystalline · Band gap · Photocatalysis

Introduction

Nano-TiO_2 materials as photocatalysts have been studied widely for potential application in decontamination of the environment. The photocatalytic properties of TiO_2 powders depend on light absorption. However, TiO_2 is activated only in the ultraviolet region, which restricts its application under natural light conditions. A large number of efforts have been made to enhance the photocatalytic property of TiO_2. For example, short band gap semiconductors CdS [1–4], CdSe [5], PbS [6], and Fe_2O_3 [7], V_2O_5 [8], Bi_2S_3 [9], SnO_2 [10–12] have been used as additives, nitrogen [13] and sulfur [14] have been added to reduce the band gap energy of TiO_2, and noble metals Pt–Ru [15] and Au [16, 17] have been added as catalysts.

H. Y. He (✉)
Key Laboratory of Auxiliary Chemistry & Technology for Chemical Industry,
Ministry of Education, Shaanxi University of Science and Technology, 710021 Xi'an, China
e-mail: hehy@sust.edu.cn

Sulfur doping can extend the light absorption to visible light and is non-poisonous to the environment. Thus, sulfur-doped TiO_2 powder has been widely studied as a photocatalyst. The sulfur doping content of TiO_2 powder is associated with the synthetic process and can substantially affect the photocatalytic activity of the powders. To improve the photocatalytic activity of S-doped TiO_2 powder, increasing the sulfur doping content has become a key topic. New efficient and economic synthetic processes obviously need to be developed. The solvothermal process may be relatively effective in wet methods because small amounts of elemental oxygen in the solvothermal solution theoretically favors formation of titanium sulfide. In this paper we report:

1 solvothermal syntheses of sulfur-doped TiO_2 powder and TiS_2 powder; and
2 comparison of the photocatalytic activity of the synthesized powders.

Experimental

The S-doped TiO_2 powders were synthesized with a starting composition of 0.004 mol titanium sulfate ($Ti(SO_4)_2$) and 25 mL ammonium sulfide ($(NH_4)_2S$). The TiS_2 was synthesized with a starting composition of 0.008 mol amorphous TiS_2 and 0.008 mol sodium thiosulfate $Na_2S_2O_3{\cdot}5H_2O$ and 25 mL *n*-heptane. The amorphous TiS_2 was synthesized by reaction between titanium sulfate ($Ti(SO_4)_2$) and sodium sulfide (Na_2S) in aqueous solution. Two starting compositions were reacted in two 40-mL autoclaves at 200 °C for 4 h. Cooling was performed at the furnace. The reaction products were filtered and then washed repeatedly with distilled water. As washed powders were dried at 100 °C for 3 h. The two powders appeared yellowish brown and dark brown, respectively.

Characterization of the powders

Phase identification of the S-doped TiO_2 and TiS_2 powders was conducted at room temperature using X-ray diffractometry (XRD; $CuK_{\alpha 1}$, $\lambda = 0.15406$ nm; model no: D/Max-2200PC; Rigaku, Japan). The phases and particle sizes of the powders were determined with the Jade5 analytical software that was provided with the X-ray diffractometer. The morphology and X-ray energy-dispersive spectra (EDS) of the powders were analyzed using scanning electron microscopy (SEM, model no: JXM-6700F; Japan).

In this study, methyl orange was used as a photocatalytic substrate to study photodegradation on the S-doped TiO_2 and TiS_2 powders. Photodecomposition experiments were performed in glass beakers. In each experiment, 100 mL methyl orange solutions at a concentration of 1×10^{-6} M were added to 50 mg S-doped TiO_2 and TiS_2 powders and dispersed with a KQ-50E ultrasonic generator. Sunlight was used as light source. The absorption spectra of methyl orange solutions before and after irradiation for different times were measured on a WFZ-900D4 spectrophotometer.

The concentrations of methyl orange solution (C) were calculated using absorption intensities before and after irradiation for different time (I_0 and I) according to:

$$C = \frac{I}{I_0}$$

The UV–visible adsorption spectra of the powders dispersed in acetylacetone were also measured in a range 190–900 nm.

Results and discussion

X-ray diffractometry was used to determine the phase of the synthesized powders. The results showed that the powder solvothermally synthesized with titanium sulfate and ammonium sulfide is the TiO_2 phase with an anatase structure (Fig. 1a). The lattice constants calculated by XRD data analysis are $a = b = 3.7936$, and $c = 9.5168$, which are larger than $a = b = 3.79$, and $c = 9.51$ for the pure anatase. This could indicate that sulfur anion partially substituted the oxygen anion and entered the anatase crystal lattice because of the larger radius of the S^{2-} anion (1.84) than that of O^{2-} anion (1.40). This is also consistent with the yellowish brown color of the powder. The TiS_2 powders synthesized by aqueous reaction between titanium sulfate and sodium sulfide and by the following solvothermal process all have an amorphous structures (Fig. 1b, c). However, the color of the TiS_2 powder changes from a white to a dark brown in the solvothermal process, which could be explained by the formation of metacrystalline TiS_2.

The SEM micrographs of the powders are illustrated in Fig. 2. The powder solvothermally synthesized with titanium sulfate and ammonium sulfide shows uniform rode-like morphology and average grain size of 10–70 nm (Fig. 2a). The powders synthesized by the solvothermal process on the aqueous reaction product show sphere morphology and average grain size of 10–100 nm (Fig. 2b). The X-ray energy-dispersive spectrum (EDS) of the S-doped TiO_2 powder is shown in Fig. 3, which reveal that the sulfur content of the doped powder is about 2.0 mol%.

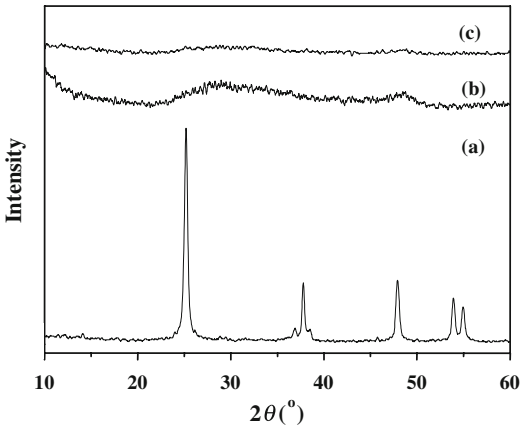

Fig. 1 XRD patterns of (*a*) the S-doped TiO_2 powder, (*b*) amorphous TiS_2, and (*c*) TiS_2 powder obtained by the solvothermal process

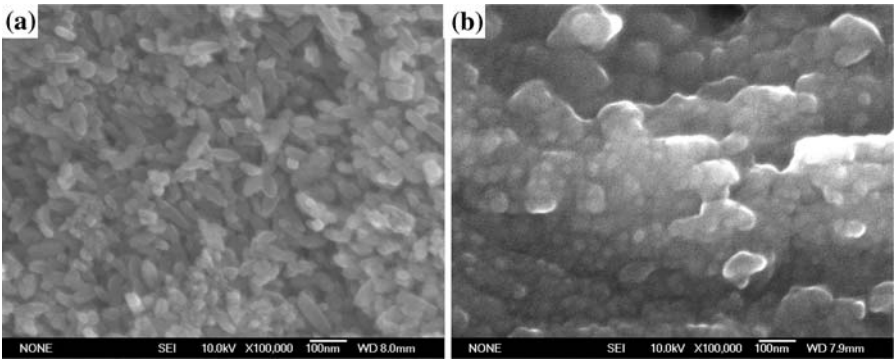

Fig. 2 SEM micrographs of **a** the S-doped TiO_2 powder, and **b** TiS_2 powder obtained by the solvothermal process

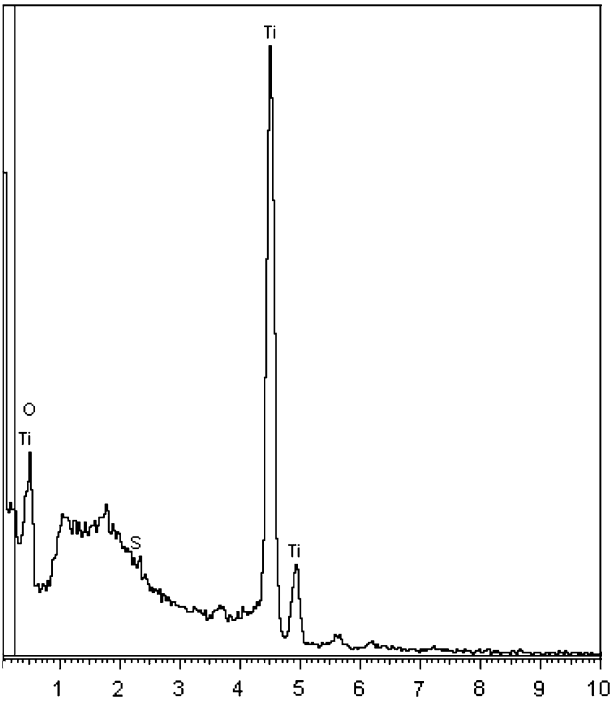

Fig. 3 X-ray energy dispersive spectrum of the S-doped TiO_2 powder

Similarly, the S-doped TiO_2 powder was synthesized by a hydrothermal process by Liu et al. [18]. This powder showed a uniform rode-like morphology but a rutile structure. The sulfur content in the powder was only 0.015 mol%. Formation of TiO_2 requires a larger chemical potential energy compared with TiS_2 because of the larger electronegativity of the oxygen atom (3.5) than that of the sulfur atom (2.5). The low oxygen content of the starting composition used in this work could be a

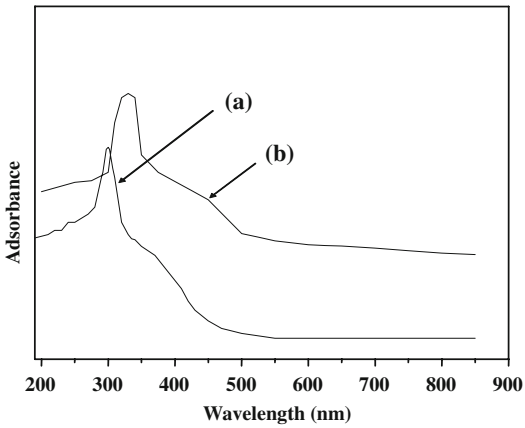

Fig. 4 Adsorption spectra of (*a*) the S-doped TiO_2 powder, and (*b*) TiS_2 powder obtained by the solvothermal process

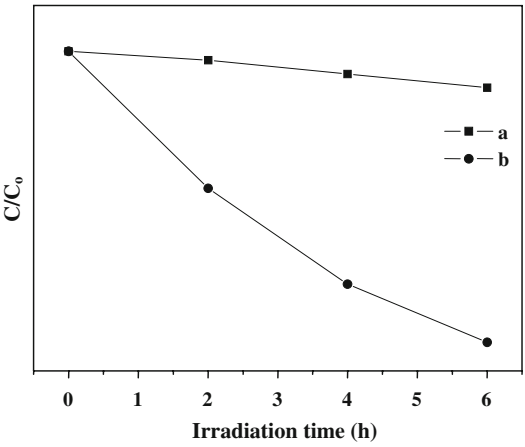

Fig. 5 Concentration variations of methyl orange solution with irradiation time on (*a*) the S-doped TiO_2 powder, and (*b*) TiS_2 powder obtained by the solvothermal process

reason fo the high sulfur content of the S-doped TiO_2 powder in comparison with the hydrothermally synthesized powder [18].

The UV–visible adsorption spectra of the powders are shown in Fig. 4. The absorption edge of the S-doped TiO_2 powder is in region of visible light of 460 nm, which corresponds to a band gap energy of 2.70 eV. Compared with the pure anatase TiO_2 (3.2 eV), the band gap of the powder is narrowed, because of the narrower band gap of TiS_2 than that of the TiO_2. The absorption edge of the TiS_2 powder shifts to the visible light region of 595 nm, corresponding to a band gap energy of 2.08 eV. Bulk TiS_2 has a band gap of about 2.0 eV [19]. This shift of 0.08 eV could be because of a quantum size effect of the powder. Except for this absorption, stronger absorption than that of the partially S-doped TiO_2 powder in the region of >595 nm could demonstrate the presence of a narrower band gap for the pure TiS_2 powder, which could be a smaller indirect band gap of 1.4 eV [19] or 1.0 eV [20, 21].

Photodegradation of methyl orange solutions on the two powders were studied in the experiments. Figure 5 shows the absorbance variations of the methyl orange solutions at $\sim$462 nm with irradiation time. It is obvious that photodegradation on the two powders increases with increasing irradiation time. Photodegradation of the methyl orange is much faster on the pure TiS_2 powders than on the S-doped TiO_2 powders, despite the larger average grain size of the former.

Conclusion

New classes of sulfur-doped TiO_2 and pure TiS_2 photocatalysts were prepared by a unique solvothermal synthetic process at relatively low temperatures. The sulfur-doped titania had a single anatase phase and a relatively small grain size.

For the samples obtained in this work, the visible-light absorbance correlated with sulfur content. The absorbance edge shifts to 595 nm for the TiS_2 powder from 460 nm for the S-doped powder. The S-doped TiO_2 powder has a significantly higher sulfur content and greater visible-light photocatalytic activity than the previously reported S-doped anatase TiO_2. The visible-light photocatalytic activity was dependent on the visible-light absorbance. The visible-light photocatalytic activity of the TiS_2 is much larger than that of the partially S-doped powder. The two powders synthesized in this work are promising visible-light-driven photocatalysts.

References

1. P.A. Sant, P.V. Kamat, Inter-particle electron transfer between size-quantized CdS and TiO_2 semiconductor nanoclusters. Phys. Chem. Chem. Phys. **4**, 98–203 (2002)
2. K.R. Gopidas, M. Bohorquez, P.V. Kamat, Photophysical and photochemical aspects of coupled semiconductors charge-transfer processes in colloidal CdS-TiO_2 and CdS-AgI systems. J. Phys. Chem. **94**, 6435–6440 (1990)
3. K.R. Gopidas, P.V. Kamat, Photoelectrochemistry in particulate systems. 11. Reduction of phenosafranin dye in colloidal TiO_2 and CdS suspensions. Langmuir **5**, 22–26 (1989)
4. D. Liu, P.V. Kamat, Electrochemical rectification in CdSe + TiO_2 coupled semiconductor films. J. Electroanal. Chem. Interfacial Electrochem. **347**, 451–456 (1993)
5. D. Liu, P.V. Kamat, Photoelectrochemical behavior of thin CdSe and coupled TiO_2/CdSe semiconductor films. J. Phys. Chem. **97**, 10769–10773 (1993)
6. N. Serpone, E. Borgarello, M. Grätzel, Visible light induced generation of hydrogen from H_2S in mixed semiconductor dispersions: improved efficiency through inter-particle electron transfer. J. Chem. Soc. Chem. Commun. 342–344 (1984)
7. W. Choi, A. Termin, M. Hoffmann, The role of metal ion dopants in quantum-sized TiO_2: correlation between photoreactivity and charge carrier recombination dynamics. J. Phys. Chem. **98**, 13669–13679 (1994)
8. S.T. Martin, C. Morison, M.R. Hafmann, The role of metal ion dopants in quantum-sized TiO_2: correlation between photoreactivity and charge carrier recombination dynamics. J. Phys. Chem. **98**, 13695–13704 (1994)
9. R. Saurez, P.K. Nair, P.V. Kamat, Photoelectrochemical behavior of Bi_2S_3 nanoclusters and nanostructured thin films. Langmuir **14**, 3236–3241 (1998)
10. I. Bedja, P.V. Kamat, Capped semiconductor colloids. Synthesis and photoelectrochemical properties of TiO_2 capped SnO_2 surfaces. J. Phys. Chem. **99**, 9182–9188 (1995)

11. K. Vinodgopal, P.V. Kamat, Enhanced rates of photocatalytic degradation of an azo dye using SnO_2/TiO_2 coupled semiconductor thin films. Environ. Sci. Technol. **29**, 841–845 (1995)
12. K. Vinodgopal, I. Bedja, P.V. Kamat, Nanostructured semiconductor films for photocatalysis photoelectrochemical behavior of SnO_2/TiO_2 coupled systems and its role in photocatalytic degradation of a textile azo dye. Chem. Mater. **8**, 2180 (1996)
13. T. Lindgren, J.M. Mwabora, E. Avendano, J. Jonsson, A. Hael, C. Granqvist, S. Lindquist, Photoelectrochemical and optical properties of nitrogen-doped titanium dioxide film prepared by reactive DC magnetic sputtering. J. Phys. Chem. B. **107**, 5709–5716 (2003)
14. T. Umebayashi, T. Yamaki, H. Itoh, K. Asai, Bandgap narrowing of titanium dioxide by sulfur doping. Appl. Phys. Lett. **81**, 454–456 (2002)
15. K. Drew, G. Girishkumar, K. Vinodgopal, P.V. Kamat, Boosting the fuel cell performance with a semiconductor photocatalyst: TiO_2/Pt–Ru hybrid catalyst for methanol oxidation. J. Phys. Chem. B **109**, 11851–11857 (2005)
16. V. Subramanian, E.E. Wolf, P.V. Kamat, Catalysis with TiO_2/Au nanocomposites: effect of metal particle size on the fermi level equilibration. J. Am. Chem. Soc. **126**, 4943–4950 (2004)
17. V. Subramanian, E.E. Wolf, P.V. Kamat, Influence of metal/metal ion concentration on the photocatalytic activity of TiO_2–Au composite nanoparticles. Langmuir **19**, 469–474 (2003)
18. H. Liu, L. Gao, (Sulfur, nitrogen)-codoped rutile–titanium dioxide as a visible-light-activated photocatalyst. J. Am. Ceram. Soc. **87**, 1582–1584 (2004)
19. H.W. Myron, A.J. Freemen, Electronic structure and optical properties of layered dichalcogenides: TiS_2 and $TiSe_2$. Phys. Rev. B **9**, 481–486 (1974)
20. A.H. Thompson, K.R. Pisharody, R.F. Koehler Jr., Experimental study of the solid solutions $Ti_xTa_{1-x}S_2$. Phys. Rev. Lett. **29**, 163–166 (1972)
21. A.H. Thompson, Electron–electron scattering in TiS_2. Phys. Rev. Lett. **35**, 1786–1789 (1975)